

# Self-Powered and Self-Functional Cotton Sock Using Piezoelectric and Triboelectric Hybrid Mechanism for Healthcare and Sports Monitoring

Minglu Zhu,<sup>†,‡,§,⊥,ⓧ</sup> Qiongfeng Shi,<sup>†,‡,§,⊥,ⓧ</sup> Tianyi He,<sup>†,‡,§,⊥</sup> Zhiran Yi,<sup>#</sup> Yiming Ma,<sup>†,‡,§,⊥</sup> Bin Yang,<sup>\*,#</sup> Tao Chen,<sup>\*,||</sup> and Chengkuo Lee<sup>\*,†,‡,§,⊥</sup>

<sup>†</sup>Department of Electrical & Computer Engineering, National University of Singapore, 4 Engineering Drive 3, 117576, Singapore

<sup>‡</sup>National University of Singapore Suzhou Research Institute (NUSRI), Suzhou Industrial Park, Suzhou 215123, China

<sup>§</sup>Center for Sensors and MEMS, National University of Singapore, 4 Engineering Drive 3, 117576, Singapore

<sup>⊥</sup>Hybrid Integrated Flexible Electronic Systems (HIFES), 5 Engineering Drive 1, 117608, Singapore

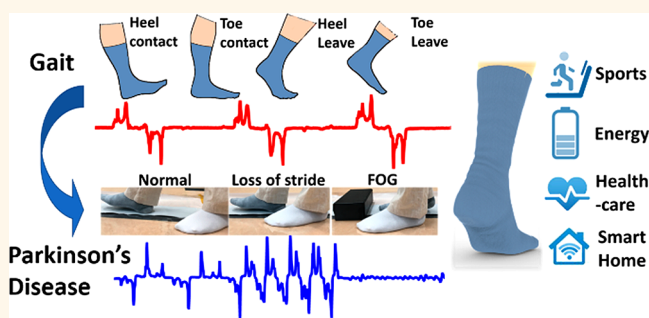
<sup>||</sup>Jiangsu Provincial Key Laboratory of Advanced Robotics, School of Mechanical and Electric Engineering, Soochow University, Suzhou 215123, China

<sup>#</sup>National Key Laboratory of Science and Technology on Micro/Nano Fabrication, Department of Micro/Nano Electronics, Shanghai Jiao Tong University, Shanghai 200240, China

## Supporting Information

**ABSTRACT:** Wearable devices rely on hybrid mechanisms that possess the advantages of establishing a smarter system for healthcare, sports monitoring, and smart home applications. Socks with sensing capabilities can reveal more direct sensory information on the body for longer duration in daily life. However, the limitation of suitable materials for smart textile makes the development of multifunctional socks a major challenge. In this paper, we have developed a self-powered and self-functional sock ( $S^2$ -sock) to realize diversified functions including energy harvesting and sensing various physiological signals, *i.e.*, gait, contact force, sweat level, *etc.*, by hybrid integrating poly(3,4-ethylenedioxythiophene) polystyrenesulfonate (PEDOT:PSS)-coated fabric triboelectric nanogenerator (TENG) and lead zirconate titanate (PZT) piezoelectric chips. An output power of 1.71 mW is collected from a PEDOT:PSS-coated sock with mild jumping at 2 Hz and load resistance of 59.7 M $\Omega$ . The study shows that cotton socks worn daily can potentially be a power source for enabling self-sustained socks comprising wireless transmission modules and integrated circuits in the future. We also investigate the influences of environmental humidity, temperature, and weight variations and verify that our  $S^2$ -sock can successfully achieve walking pattern recognition and motion tracking for smart home applications. On the basis of the sensor fusion concept, the outputs from TENG and PZT sensors under exercise activities are effectively merged together for quick detection of the sweat level. By leveraging the hybrid  $S^2$ -sock, we can achieve more functionality in the applications of foot-based energy harvesting and monitoring the diversified physiological signals for healthcare, smart homes, *etc.*

**KEYWORDS:** triboelectric, piezoelectric, textile, sock, sensor



Benefiting from a technology boost in terms of miniaturization and flexible materials, wearable devices have experienced enormous advancement. To further enhance the stretchability<sup>1</sup> and flexibility needed for comfortable devices that are suitable for operation on the human body, designs are proposed with distinctive structures, such as origami,<sup>2</sup> kirigami,<sup>3</sup> wavy,<sup>4</sup> and other fractal layouts.<sup>5</sup> Eventually,

research has been dedicated to realizing more intelligent devices with the aid of integrated circuits (ICs), sensing modules and

**Received:** October 31, 2018

**Accepted:** February 11, 2019

**Published:** February 11, 2019

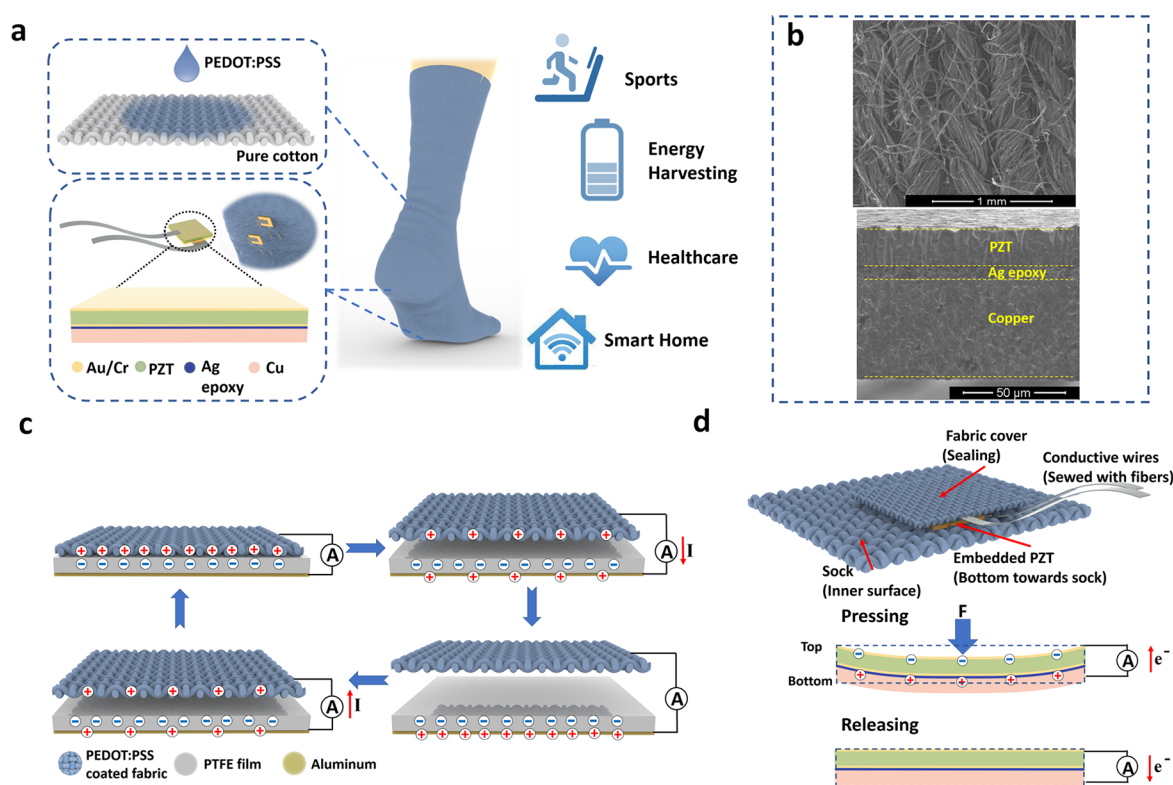


**Figure 1.** (a) Schematic of PEDOT:PSS coated triboelectric S<sup>2</sup>-sock integrated with PZT force sensors for diversified applications, with left side showing the enlarged views of TENG textile and embedded PZT sensor. Foot model is reproduced with permission from [turbosquid.com](https://www.turbosquid.com). (b) (Top) Top view of SEM image of PEDOT:PSS-coated textile. (Bottom) Cross-section view of SEM image of PZT chips. (c) Working principle of TENG sock under contact-separation mode. (d) Working principle of PZT chip and integration strategy for S<sup>2</sup>-sock.

functional materials such as flexible wrist bands<sup>6,7</sup> and electrochemical-based tattoos<sup>8</sup> for biosensors, mechanoreceptors for skin prosthesis,<sup>9–11</sup> and wearable displays.<sup>12</sup> To implement the continuous and convenient monitoring of diversified physiological signals<sup>13,14</sup> in a timely manner, the self-powered wearable devices<sup>15</sup> with hybrid mechanisms have become a major research topic, *i.e.*, to effectively combine the individual element with specific properties such as piezoelectric, thermoelectric, capacitive, photovoltaic, triboelectric, and electromagnetic.

The collaboration of individual components from hybrid wearable device strengthens the energy-harvesting capability and enriches the sensing of a variety of signals. Zhang *et al.*<sup>16</sup> proposed self-powered temperature–pressure dual-parameter sensors based on thermoelectric and piezoresistive effects. Leung *et al.*<sup>17</sup> introduced a flexible and self-powered photo-detector by integrating triboelectric nanogenerator (TENG). A piezoelectric–pyroelectric-based hybrid nanogenerator was developed by Lee *et al.*<sup>18</sup> Hence, a wearable device with combinational functions is a promising solution for a compact smart system.

In terms of portability and comfort, self-functional textiles for clothes, socks, or gloves have become a popular research topic for wearable devices,<sup>19–23</sup> and smart textiles are aimed to be not only more comfortable but also multifunctional, *i.e.*, cognition, adaptation, or integration.<sup>24–28</sup> Within the present self-powered sensor, one of the major trends is to use TENG fabrics to scavenge energy<sup>29,30</sup> and detect various types of sensing signals.<sup>31–33</sup> Yu *et al.*<sup>34</sup> reported core–shell yarns based TENG clothes as a power source. Lin *et al.*<sup>35</sup> proposed a self-powered TENG sleeping monitoring system using an array of

conductive fibers. On the other hand, it is universally accepted that the output of TENG will be affected by the presences of humidity level and ionic contents.<sup>36,37</sup> While Wang *et al.*<sup>38</sup> have developed a water–air TENG sensor to compensate for the influence of humidity on the triboelectric output and a water energy harvester fabricated by hydrophobic cellulose oleoyl ester nanoparticles was reported by Xiong *et al.*,<sup>39</sup> approaches of minimizing the triboelectric output fluctuation due to humidity variation in different usage scenarios remain an important research direction.

A hybrid system is then required as a compensation, and the use of a piezoelectric element as a sensor has been studied extensively in the detection of diversified signals, such as force, and chemicals *etc.*<sup>40–48</sup> and shows promising features as a TENG where both can transform mechanical input, *i.e.*, the mechanical energy, into electrical output, *i.e.*, the electrical energy.<sup>49,50</sup> There are reported approaches of integrating both mechanisms into one device,<sup>51–54</sup> but most of them still focus on power enhancement by a hybrid energy harvester. In this paper, we propose a solution of utilizing piezoelectric elements to compensate for the attenuation of triboelectric output.

Currently, the rapid expansion of the Internet of Things (IoT) reveals the essential requirements of smart textiles with power generation and diversified signal sensing by hybrid mechanisms. Human motions can generate a few hundred watts of kinetic energy in total from different parts, among which foot activity is one of the major sources. In addition, the gait also contains valuable information regarding healthcare and personal identification,<sup>55–58</sup> which eventually became the motivation for developing insoles with energy-harvesting and -sensing abilities.<sup>59–62</sup> However, to the best of our knowledge, except for

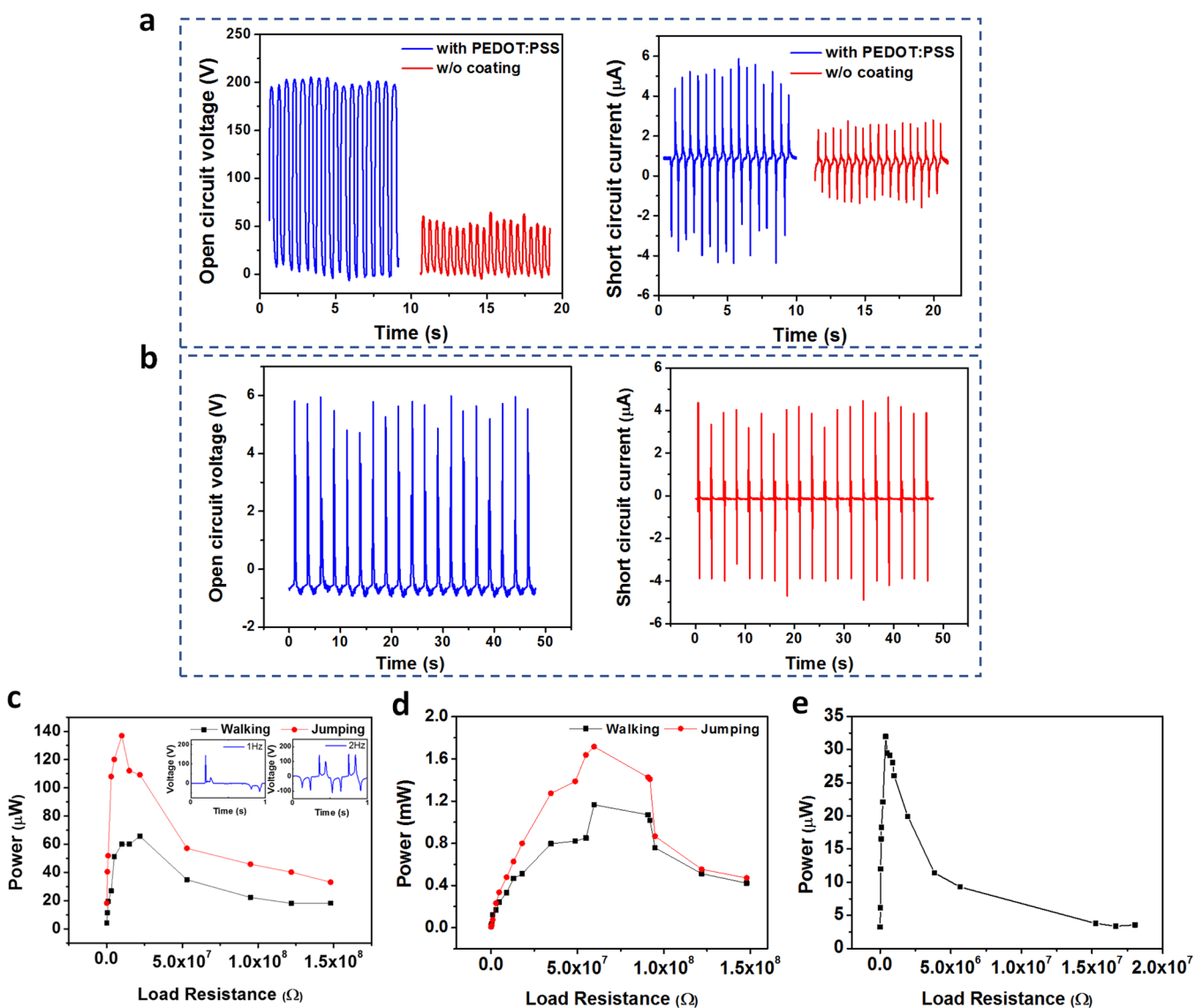


**Figure 2.** (a) Comparisons of open-circuit voltage and short circuit current between PEDOT:PSS-coated sock and original sock under contact separation mode shown in Figure 1c. (b) Open-circuit voltage and short-circuit current of PZT chip with connection shown in Figure 1d. (c, d) Power output against the external loading resistance with and without shoes. The maximum powers are 66 and 137  $\mu\text{W}$  at 20 M $\Omega$  for walking (at 1 Hz) and jumping (at 2 Hz) with shoes as well as 1.17 and 1.71 mW at 59.7 M $\Omega$  for walking and jumping without shoes (with PTFE + aluminum sheet), respectively. (e) Power curve of PZT chip under the external loading resistance ranges from 0.5 to 148 M $\Omega$ , with a maximum power of 32  $\mu\text{W}$ .

the attachment of a functional component,<sup>63</sup> there is no reported research on direct utilization of the sock itself as both energy harvester and multipurpose sensors. Unlike the insole, the sock can still be functional for indoor scenarios, particularly at home, where shoes are not necessary. Walking patterns, sweat levels, or motion sensing of those diversified signals can be easily conducted through several mechanisms for sports, healthcare monitoring, and rehabilitation applications, *i.e.*, the evaluation of Parkinson's disease, which may not be effective *via* routine examination at clinic. Further improvements the functionalities can also be fulfilled by additional coatings or components on TENG socks, such as detection of chemicals released from human body,<sup>64–66</sup> actuators like neural stimulation,<sup>67</sup> capacitors,<sup>68</sup> antibacterial,<sup>69</sup> controller,<sup>70</sup> and drug delivery.<sup>71</sup> Hence, this hybrid self-powered sensor offers a desirable platform for wearable sensors.

Here, we report a self-powered and self-functional sock ( $S^2$ -sock) based on poly(3,4-ethylenedioxythiophene) polystyrene-sulfonate (PEDOT:PSS) coated TENG textile with the integration of lead zirconate titanate (PZT) piezoelectric sensor, as illustrated in Figure 1a. PEDOT:PSS, as a commercialized conductive polymer, is widely adopted as a coating or printable electrode with possession of high conductivity<sup>72</sup> as well as good stability in terms of mechanical deformation and chemicals.<sup>73</sup> PZT is also a well-known piezoelectric material with an excellent piezoelectric constant of about  $d_{31} = -200 \text{ pC N}^{-1}$  in the bulk ceramic form. To integrate the 20  $\mu\text{m}$  thin PZT chips into the  $S^2$ -sock, another 50  $\mu\text{m}$  copper substrate was bonded together (Figure 1b) to enhance the ductility and optimize the mechanical neutral plane. Besides the basic energy harvesting capability, a facile fully coated sock can generate the featured waveforms which offer a convenient method for walking pattern recognition and motion tracking of individuals for home care

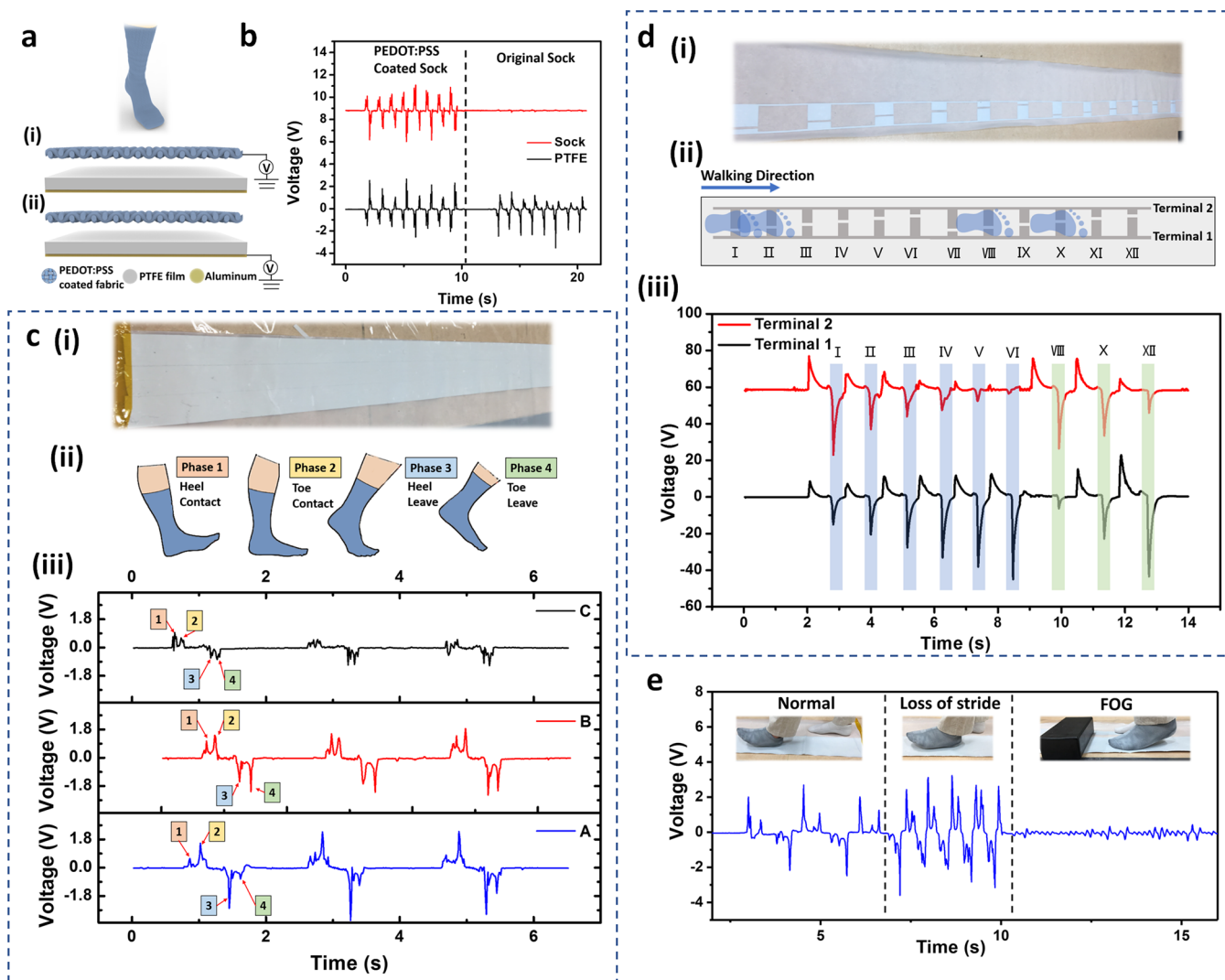


**Figure 3.** Experimental results of monitoring indoor activities (without shoes) with a simple fully coated  $S^2$ -sock. All signals are collected from the PTFE side, with the positive peak representing contact and negative peak representing separation. (a) Schematic of coated  $S^2$ -sock and two possible electrical connections for single electrode mode TENG: (i) sock connection and (ii) Al/PTFE connection. Connection (ii) is used in this section. Foot model is reproduced with permission from [turbosquid.com](http://turbosquid.com). (b) Voltage signals of both PTFE and sock collected from walking on the PTFE path; the signals of original sock are compared. (c) (i) Photo of PTFE films and full aluminum-covered electrodes; (ii) schematics of four phases of a typical contact cycle and corresponding signals: (1) heel contact, (2) forefoot/toe contact, (3) heel leave, and (4) forefoot/toe leave; (iii) output signals of pattern recognition of normal walking (right foot) for three participants, (A) 90 kg male, (B) 70 kg male, and (C) 60 kg male. The phases are labeled on the corresponding peaks of the output signals. (d) (i) Photo of PTFE films and six couples of designed aluminum electrodes with two terminals and two cycles, (ii) schematics of motion tracking based on the designed path with the area ratio of 6:1, 5:2, 4:3, 3:4, 2:5, and 1:6, labeled as I–VI and VII–XII, with two different walking paces, (iii) output signals of motion tracking from two terminals—the first and second cycle are highlighted with blue and green. (e) Mimetic walking pattern of Parkinson's disease patient under three conditions: normal, loss of stride, and freezing of gait (FOG).

applications. Second, as a concept of sensor fusion, a quick evaluation of sweat level was also demonstrated by the TENG + PZT sensor through the output generated simply from direct mechanical contact. The modified multisectional PEDOT:PSS pattern and embedded thin PZT chips enable the gait sensing and contact force analysis. Briefly speaking, we have successfully turned the conventional sock into a carrier with the capability of sensing signals and scavenging the wasted energy, a joint function of two sensors acting as the complementary parts of each other to balance the individual weaknesses associated with sensing mechanisms. This platform presents the feasibility of continuous exploration of incorporations with other wearable techniques.

## RESULTS AND DISCUSSION

The inner surface of shoes was covered by PTFE film and an aluminum electrode connected to sock as depicted in Figure 1c, and PZT chips are integrated at the inner surface of the sock (Figure 1d). To examine the performance of energy harvesting, a series of characterizations were conducted by regular jumping at 2 Hz frequency while wearing shoes (Figure 2a). To evaluate the enhancement from PEDOT:PSS coating, the open-circuit voltage and short-circuit current were compared between the coated sock and original sock, and the obtained average voltage of 196 and 55 V and the average current of 4.5 and 2.3  $\mu\text{A}$  are achieved, respectively. The results prove the superiority of a PEDOT:PSS-coated sock in terms of energy harvesting, due to

the better conductivity for charge transmission. The open-circuit voltage output of 196 V from the contact-separation mode against 130 V from a single electrode mode (see Figure S2 in the Supporting Information) indicates that the contact-separation mode is more suitable for energy harvesting in shoes. Additionally, two important environmental factors, temperature and humidity, were evaluated regarding the influences on TENG output (see Figure S4 in the Supporting Information). The output amplitude shows 20% decrement from 50% to 90% relative humidity (RH) and 10% decrement from 50 to 10 °C. These fluctuations would not bring severe issues to waveform-based sensing functions. In this study, the humidity and temperature were kept at 70% RH and 25 °C if not specified.

The maximum output powers of a single sock under various scenarios were tested by changing the external load resistances from 0.5 to 148 M $\Omega$ . For in-shoe conditions in Figure 2c, the output powers of 66 and 137  $\mu$ W were generated based on 1 Hz walking and 2 Hz jumping under loading resistance of 10 M $\Omega$ , respectively. In the case of indoor use, when stepping on the PTFE film placed on the ground with bare sock, maximum powers of 1.17 and 1.71 mW were obtained accordingly under the loading resistance of 59.7 M $\Omega$  in Figure 2d, which gives the power density of 11  $\mu$ W/cm<sup>2</sup> under the contact area of about 150 cm<sup>2</sup>. The characterized relationship between output voltage and contact area was also performed by force gauge (see the results of Figure S4b in the Supporting Information). Noticeably, due to the variation of the size of PTFE film, the impedance of the whole system was shifted, and this huge boost of power generation is attributed to the increasing of separated distance compare to that of wearing shoes. For a PZT chip, the characteristic open-circuit voltage and short-circuit current are shown in Figure 2b, and a maximum output power of 32  $\mu$ W per chip (5 mm  $\times$  5 mm) can be harvested under 0.4 M $\Omega$  load resistance and 12 N at 1 Hz frequency from Figure 2e, indicating a maximum power density of 128  $\mu$ W/cm<sup>2</sup>. By considering the output power from those reported smart textiles, *i.e.*, 15.38  $\mu$ W/cm<sup>2</sup> from silver and poly(ethylene terephthalate) (PET) based triboelectric textile<sup>74</sup> and 13  $\mu$ W/cm<sup>2</sup> from cotton and nylon based textile,<sup>75</sup> the as-fabricated S<sup>2</sup>-sock provided the comparable performance. Furthermore, as an advantage regarding the substrate, we simply transformed this conventional cotton sock into a triboelectric energy harvester. This easy fabrication process solves the problems associated with introducing other fabric materials, *i.e.*, comfort. Compared to the insole, the duration of wearing socks can be much longer and, hence, compensate for the drawback of power density. In addition, another key contribution of the S<sup>2</sup>-sock is to offer a platform for those potential wearable devices through several approaches: (1) using the triboelectric effect to incorporate with other functional materials for realizing more application (*i.e.*, temperature and chemical sensing), (2) possibly using the conductive cotton fabric as a connector *via* inject printing technique, and (3) partially supplying the required power for the attached electronic system (*i.e.*, microprocessor and transmitter).

For the indoor scenario with bare socks worn at home as illustrated in Figure 3a, the capability of pattern recognition and motion tracking is preferred to facilitate the homecare solutions of IoT. In Figure 3b, a comparison test was conducted to verify the importance of PEDOT:PSS-coated socks for achieving this walking pattern recognition. The output from original sock shown almost no response to any motion, and the signal from PTFE terminal was also degraded. Therefore, the PEDOT:PSS

coating is crucial to S<sup>2</sup>-socks for realizing a series of functions with a certain quality.

To obtain these specific triboelectric signals during contact with better quality, the smart paths with two designs shown in Figure 3c,d were prepared from PTFE films and aluminum electrodes. The full aluminum-covered path demonstrated the walking pattern recognition functions. Typically, a complete foot-ground contact sequence for walking can be decomposed into four phases in Figure 3c (ii). On the basis of the data from the regular walking of three participants, the distinguishable signal patterns corresponding to each of them are observed as shown in Figure 3c (iii). These four phases are labeled alongside the voltage output peaks in the first cycle. The amplitude of peaks for phase 1 and 2 reveals the information regarding the speed-based contact force exerted from heel and forefoot. The time interval between phase 1 and 2 depends on the contact angle of foot against the ground, so that the smaller interval indicates the lower angle. The combined characters are usually distinctive within a certain group of people, *i.e.*, family members. In order to characterize the variations from different participants, *e.g.*, walking style, weight, and foot size, as well as the variations from environmental humidity, we conducted the experiments for signal comparison (see Figure S5 in the Supporting Information). In terms of output amplitude, change of humidity and foot size (contact area) may result small fluctuations, which are in line with the force gauge tests (see Figure S4 in the Supporting Information), and the weight differences show no obvious effect on signal intensity due to the low force requirement of full contact of sock fabric. As the sensing capabilities are achieved through the identification of waveform pattern, the minor variation of amplitude will not affect the functions. Moreover, through the machine learning process, the reliable database gathered from daily activities enables the smart home function by identifying the recorded or unknown patterns.

By further modifying the aluminum electrode on PTFE sheet, a sequence of six combinations of ascending or descending areas was prepared in two cycles, with a total length of 2.4 m, and marked from I to VI and VII to XII in Figure 3d (ii). Additionally, the design of two terminals can compensate the missing of stepping on relatively small areas. As the charge generation is affected by the contact area,<sup>76</sup> the similar trend of voltage signals was detected consistently with the designed configuration when walking through the path, either ascending or descending (Figure 3d (iii)). This feature enables the recognition of walking direction, speed, and distance. For instance, the signals from I to VI of terminal 1 revealed the direction of walking toward right side for 1.2 m within 6 s, since the sudden drop of signal (*i.e.*, VI to VIII) indicates the completion of the previous cycle. Meanwhile, although both walking toward the left and the completion of a cycle are all generating the descending output for terminal 1, these two special cases still can be differentiated according to the waveform shape of single peak. Moreover, the path can maintain its functionality even for walking with larger pace, as long as two steps at least, fell into the same cycle, such as VIII, X, and XII, with three ascending outputs still tracking the direction clearly (see video S1 in the Supporting Information). The much larger voltage in this demonstration was obtained by using a 100 M $\Omega$  high voltage probe for better impedance matching to get more accurate output correspondence against the different contact areas.

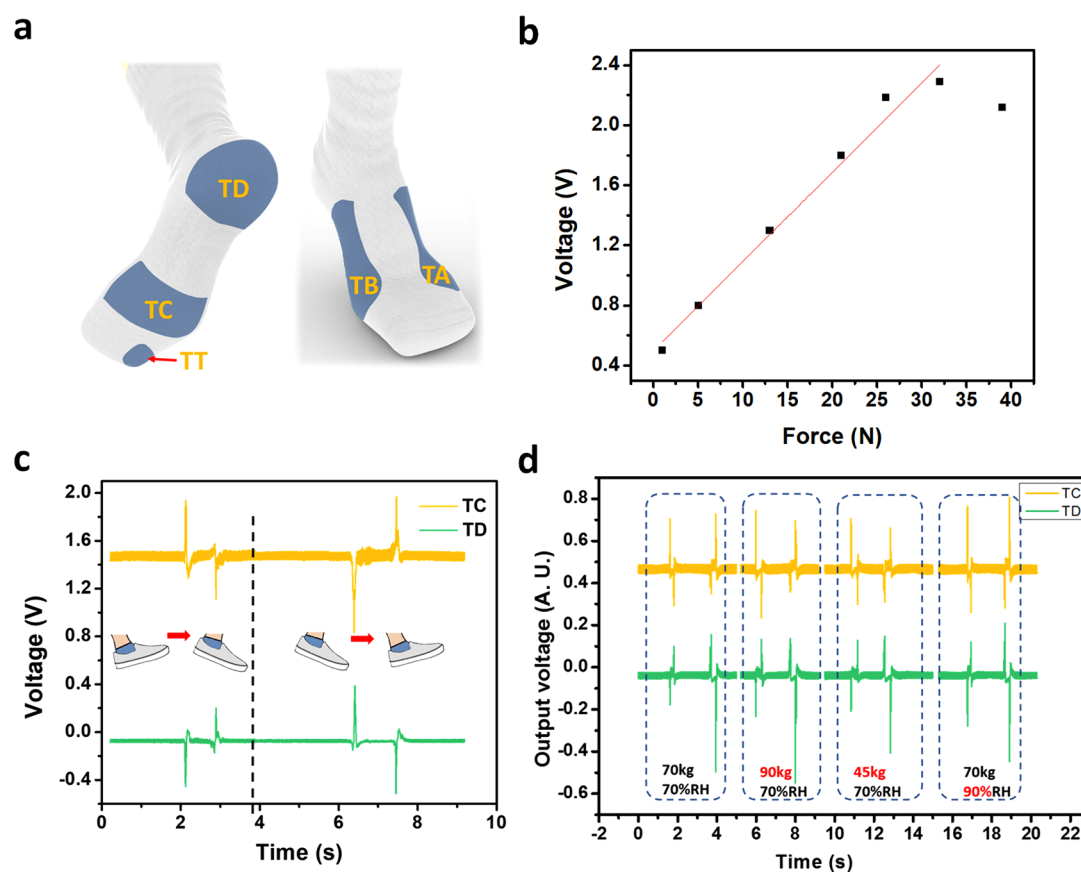


**Figure 4.** Experimental results of multisectonal PEDOT:PSS-coated  $S^2$ -sock (in shoes) with connection (i) in Figure 3a. (a) Schematic of multisectonal coating of  $S^2$ -sock. The coating areas act as sensors of corresponding region: left instep, right instep, forefoot, heel, and big toe, labeled as “TA”, “TB”, “TC”, “TD”, and “TT”, respectively. Foot model is reproduced with permission from turbosquid.com. (b) Output voltage under increasing force of TENG sensor “TT” at big toe, with the calibration of resistive force sensor “FlexiForce”. (c) Gait characterization with typical voltage signals under the contact sequences of two motions, forward: heel contact  $\rightarrow$  forefoot contact, backward: forefoot contact  $\rightarrow$  heel contact. All signals are collected from the sock, with the positive peak represents separation and negative peak represent the contact. (d) Comparison of TENG gait characterization with different weights (45, 70, and 90 kg) and humidity levels (70% RH and 90% RH).

As a typical application of healthcare by activities monitoring, Parkinson’s disease (PD), a progressive nervous system disorder which significantly affects the movement of a patient, is extensively studied. However, PD is difficult to evaluate in a routine clinical examination since it is usually triggered by special and uncertain scenarios. Hence, the requirement of continuous monitoring of PD patients at home is important. Among various measurable physiological signals,<sup>55,77,78</sup> freezing of gait (FOG), which refer to the block of movements when encountered with turning, or trying to overcome the obstacles,<sup>79</sup> can be detected by the walking pattern. However, most triboelectric gait sensors are still integrated into the insoles.<sup>60</sup> In this work, the  $S^2$ -sock was tested for detecting the mimetic motions of PD, as shown in Figure 3e (see video S2 in the Supporting Information). According to reported studies,<sup>80</sup> there was a loss of stride length prior to FOG represented in terms of the decreased time interval between output signals. Thereafter, the symptom of shaking leg caused by FOG as the attempt to overcome the obstacle was also identified through the frequent and irregular oscillation of output voltage within a small amplitude. To further assess the stability, the temperature and humidity were changed individually, and the obtained data indicate that both of the influences are almost negligible (see Figure S6b in the Supporting Information). In general, by a

simple full coating, the  $S^2$ -sock not only can scavenge the mechanical energy but also enables appliance control and activities monitoring associated with specific users, such as the elderly or a child who is identified through the distinctive walking pattern.<sup>77–82</sup> Through the machine learning process, this sock can be a promising technique for precise pattern recognition and activity monitoring, which is worth further study to improve the accuracy and repeatability of measured data.

When considering the multisectonal coating shown in Figure 4a, the  $S^2$ -socks are able to demonstrate the possibilities of gait sensing, since the full coating sock cannot differentiate the contacting points. Four sensing units labeled as “TA”, “TB”, “TC”, and “TD” are chosen to perform the basic detection about the motion directions. In addition, a big toe sensor “TT” was demonstrated as a TENG force sensor for speed-based impact force sensing with the approximate data giving sensitivity of 0.06 V/N (Figure 4b), which is sufficient for walking pattern recognition or gait sensing.

Under indoor scenarios, where we assume the scene with bare sock, by measuring the output of two sole sensors “TC” and “TD” simultaneously, the featured signals of pure heel and toe contact were characterized as illustrated in Figure 4c (see video S3 in the Supporting Information). Because of the different

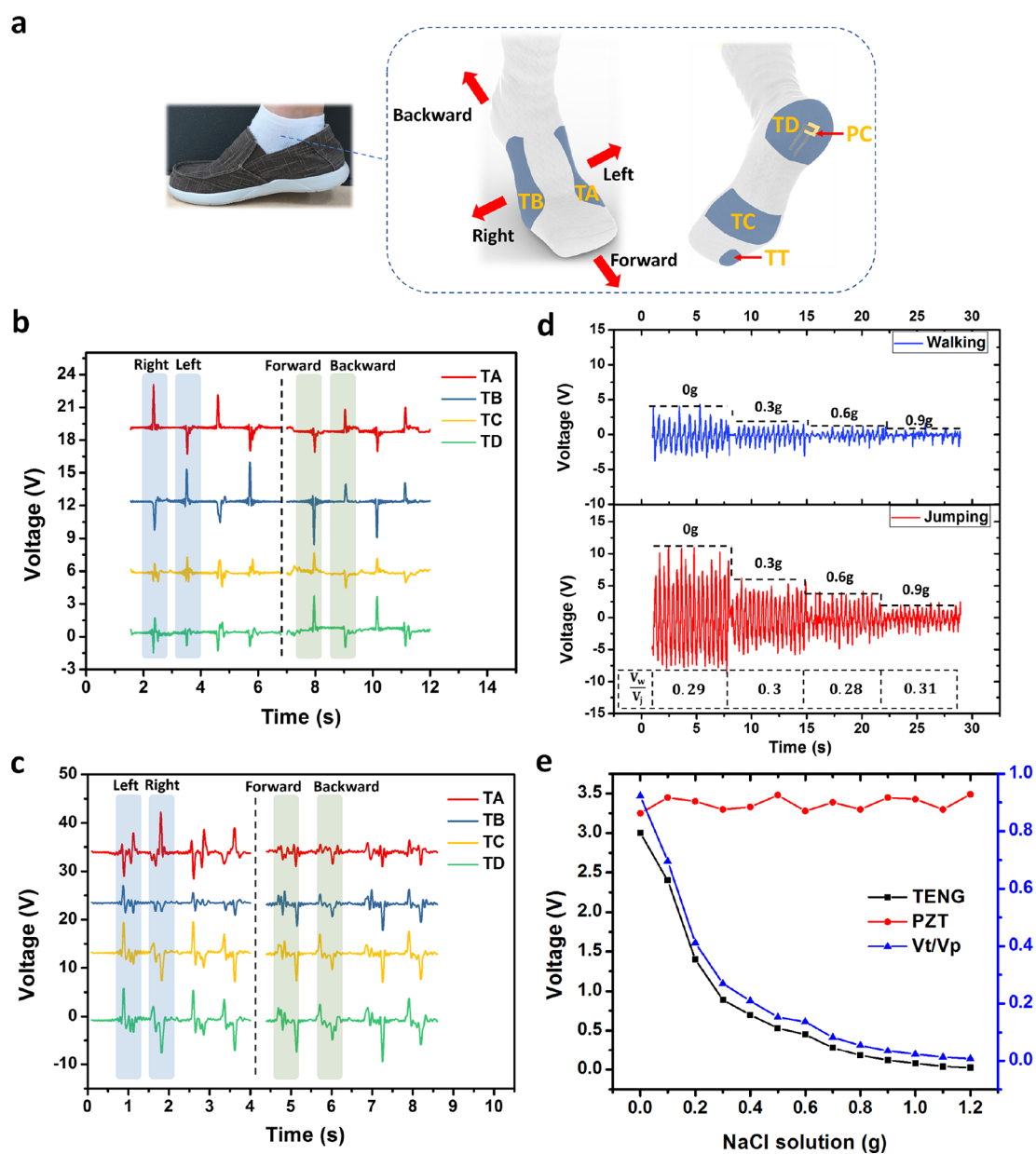


**Figure 5.** Experimental results of outdoor activities (in shoes). All signals are collected from a sock with the connection (i) in Figure 3a; the negative peak represents contact and positive peak represents separation. (a) Schematic of tested motion directions for both of sliding and walking scenarios; TENG and TENG + PZT sweat sensors (“TD” and “PC”). Foot model is reproduced with permission from [turbosquid.com](https://www.turbosquid.com). (b) Voltage signals from four TENG sensors under sliding motion; typical signals are shaded with blue and green. (c) Voltage signals from four TENG sensors under normal walking. (d) TENG output under increasing amount of 0.9 wt % NaCl solution (labeled) delivered through spray (0.1 g/spray), generated from walking and jumping,  $V_w/V_j$  represent the positive voltage ratio of two activities at each sweat level. (e) TENG sweat sensor with PZT reference sensor, blue curve represents the voltage ratio of TENG sensor over PZT sensor at each sweat level.

contact sequence between moving forward and backward (*i.e.*, forward: heel contact → forefoot contact, backward: forefoot contact → heel contact), the motion direction is identified. Similarly, the variations of different participants and environmental humidity were tested as shown in Figure 4d, and all of the signals indicate the good stability of output.

In the case of outdoor activities with shoes wearing, the physiological signals generated from foot, either physical or chemical, are always interesting aspects for medical and sports applications, such as the gait sensing mentioned in Figure 4 and sweat detection. Due to the full coverage of the  $S^2$ -sock by the shoe, all of four units of TENG (“TA”, “TB”, “TC”, and “TD”) together with the inner PTFE surface of the shoe can be

functionalized as a complete gait sensor (Figure 5a). As illustrated in Figure 5b, for left sliding, sensor “TA” experienced contact force which gave a negative peak, whereas sensor “TB” was separated from PTFE film and resulted in a positive peak. The reversed features of signals were observed for right sliding. In contrast, the continuous contact of insole sensors “TC” and “TD” generated only small signals during sliding, which are insignificant for identifying left or right sliding. For forward and backward sliding, “TA” and “TB” were contacted or separated at the same time and generated both negative or positive, respectively. Moreover, for normal walking, the signals are shown in Figure 5c, according to the features of marked output from “TC” and “TD”, and both forward/backward and left/right

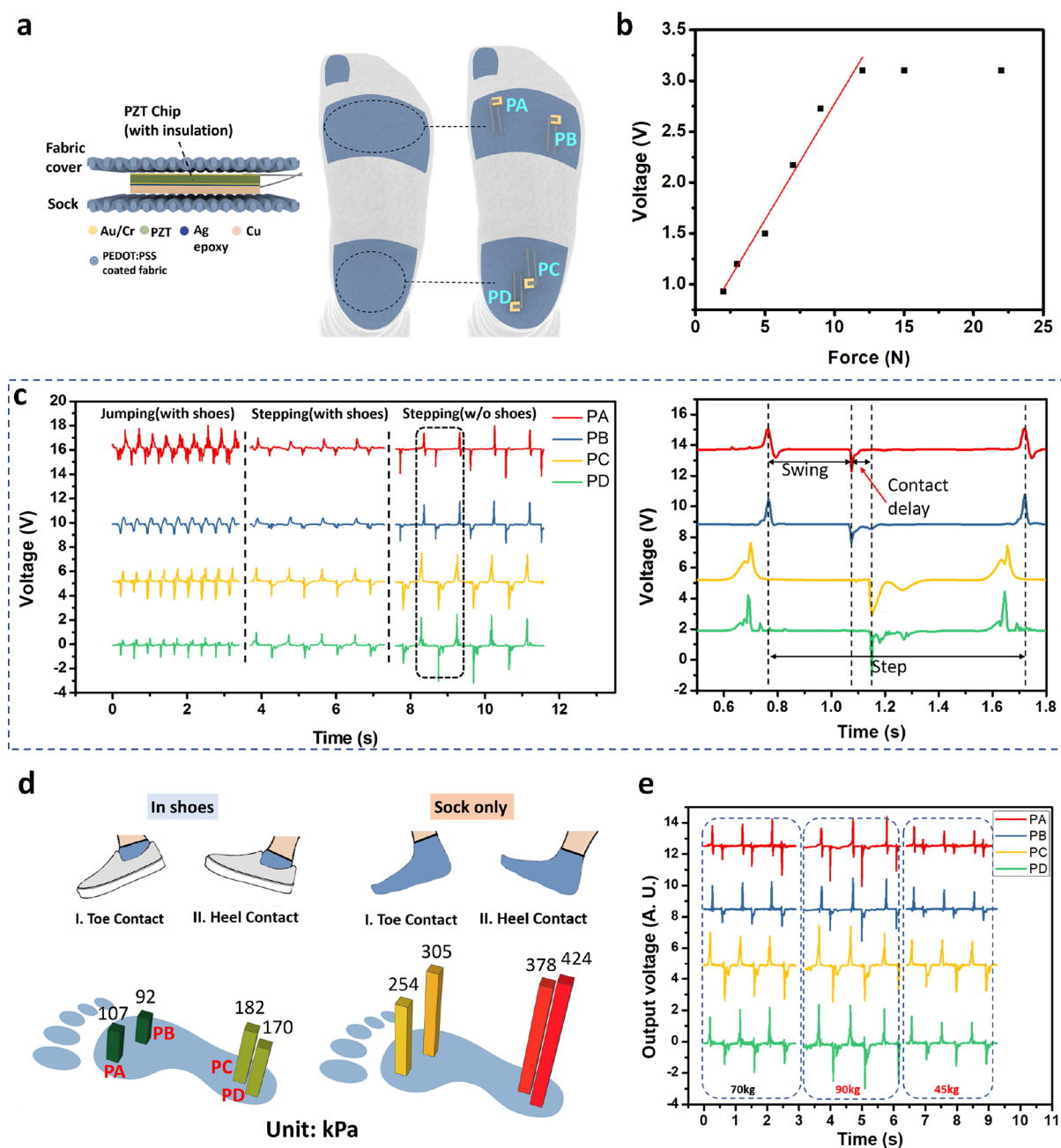


**Figure 6.** (a) Schematic of embedded PZT force sensors, labeled as “PA”, “PB”, “PC”, and “PD”. Foot model is reproduced with permission from [turbosquid.com](https://www.turbosquid.com). (b) Calibration curve of output voltage against force done by force gauge; slope of linear fit represents the sensitivity. (c) Voltage signals under three conditions: jumping with shoes, stepping with shoes, and stepping without shoes; the detailed information on one cycle in terms of time domain is enlarged at right. (d) Pressure mapping of in shoes and sock only conditions based on the measured voltage output from (I) toe contact and (II) heel contact and the force calibration curve. (e) Comparison of PZT pressure sensing with different weights ((A) 90 kg male, (B) 70 kg male, and (C) 45 kg female).

walking can be identified. Referring to the single peak signals in Figure 4c, these additional peaks came from the minor interactions between the sock and the inner surface of shoes during foot swing (see videos S4 and S5 in the Supporting Information). To further investigate the influences of environmental humidity, temperature, and weight variations, the corresponding experiments were conducted (see Figures S4–S9 in the Supporting Information). Generally, those factors show only insignificant impacts (less than 10%) on the output intensities, as compare to foot size, and TENG sensors can still

achieve all the functions with good quality and long-term stability (see Figure S8 in the Supporting Information).

Human sweat is a key indicator related to health status and training intensity. A proper monitoring of sweat level is desirable for detecting the abnormalities or the intensity of exercises. However, there is a lack of study on sweat sensing so far by using socks directly. Jao *et al.*<sup>63</sup> reported a chitosan-based humidity resistor attached on the sock, where the output voltage across the resistor is measured as a function of humidity. They also designed an arch shape TENG device, based on triboelectric output from PDMS/fabric (chitosan-glycerol as the electrode)

contact and separation, to demonstrate the feasibility of detecting concentration of sodium chloride (NaCl) solution in the fabric with saturated water content (by soaking).

On the other hand, Taylor *et al.* report that the NaCl concentration of sweat generated from body is relatively stable.<sup>83</sup> Considering the scenario of wearing socks in which the foot may generate sweat when they wear shoes, and not much sweat generated by foot if the user worn socks in open environment, we developed a self-functional sock based sweat sensor to realize straightforward and timely detection of sweat level by sensing the TENG output attenuation along with the volume variation of NaCl solution at relative constant concentration in this paper. Furthermore, we consider that the water evaporation rate of sweat inside shoes is limited. Specifically, the presence of water and ion content affects the triboelectric output through the deterioration of triboelectricity preservation and contact electrification on the surface.<sup>36,37</sup> It is then feasible for TENG to conduct qualitative analysis of foot sweating. Two configurations were then proposed for testing: individual TENG and TENG + PZT sensors as shown in Figure 5a (“TD” and “PC”). For individual TENG sweat sensing (Figure 5d), the output voltage decreases as the amount of sweat increases, in a segmental form. Because human sweating is a relative slow and continuous process, which allows the output of TENG maintains at a certain level within a short period of time, the TENG can offer general information about the sweating status by referring to the previous output with a proper sampling period. Nevertheless, the drawbacks of this approach are the difficulty of obtaining the absolute data based on dry condition, and the force applied to TENG may fluctuate dramatically due to the inconsistency of human activities. These are the most critical aspects in terms of practical application and still remain challenge to relevant researches. Therefore, the encapsulated PZT chip as a piezoelectric material was used as a reference sensor that was free of humidity influence and self-adjustable against force for specific user or scenario. As shown in Figure 5e, the output of PZT sensor maintains at about 3.3 V during 1 Hz normal walking as the NaCl solution increases. In contrast, TENG experienced the attenuation of output voltage. For simplification of the relationship between two signals and elimination of impact force variations on the output amplitude, the ratio of TENG over PZT output is plotted against the amount of NaCl solution sprayed. On the basis of the data from Taylor *et al.*,<sup>83</sup> a typical male foot surface area (for sweat glands) is about 1100 cm<sup>2</sup> (sole: 500 cm<sup>2</sup>, dorsal: 600 cm<sup>2</sup>), with a sweat rate of about 0.24 and 0.464 mg/cm<sup>2</sup>/min at exercise, the amount of sweat generated from foot ranges from 0.264 to 0.51 g/min. Therefore, the TENG + PZT sweat sensor is possible to provide the qualitative data of sweating status. Furthermore, since sweat contains various elements, like sodium ion, potassium ion, glucose, lactate, *etc.*, the detection of these chemicals can be a noninvasive method for medical monitoring. In contrast, the gait-sensing performance will be affected in terms of intensity through the increasing sweating level. However, since the real sweating of foot is much slower than the spray used in our test, the sensing signal still can maintain the required features for analysis. Hence it is possible for S<sup>2</sup>-sock to achieve such function by coating with specific enzyme to establish a comprehensive and diversified sensing system together with gait analysis in a single TENG sock.

Most of the previous studies on piezoelectric based insole sensors were emphasized on placement of more units to enhance the accuracy of pressure mapping throughout the whole foot.

However, this dense sensor array is not necessary to be implemented in the S<sup>2</sup>-sock. For understanding of the PZT chip as a preferable force sensor, several characterizations and practical tests were conducted, including sensitivity, output power, and multipixel pressure sensing results (Figure 6a). As shown in Figure 6b, the calibration was done by force gauge and a sensitivity of 0.228 V/N (0.0057 V/kPa) was achieved, indicating the superiority against the TENG force sensor. The sensing range is up to 12 N (480 kPa). According to the literature data from Betts *et al.*,<sup>84</sup> the pressure of normal human ranges from 10 to 370 kPa (estimated peak pressure for barefoot walking), which indicates the PZT chip can be used for human foot pressure measurement.

With PZT sensors, the data of pressure distribution allow us to inspect the abnormal contact during walking for rehabilitation purpose or evaluate the training intensity to avoid the injuries. Benefitting from the high sensitivity to the mechanical force, the embedded PZT sensors in the sock can perform the pressure sensing accurately and effectively. Specifically, sensors “PA” and “PB” were placed at the forefoot, and “PC” and “PD” were placed at heel. These sensors were then tested under three conditions shown in Figure 6c. The signals illustrate the distinguishable features, where the negative and positive peak corresponds to contact and separation, respectively. For stepping, because of the buffer effect from the insole, the contact force reduced a lot after wearing shoes. During jumping, a noticeable increase of contact force at “PA” was observed due to the large impact force absorbed by forefoot for landing. After integration with the signal-processing circuit and graphic user interface (GUI), a more intuitive data of 70 kg male can be presented as Figure 6d. To verify with pressure responses based on different participants, Figure 6e shows the output signal variations for barefoot walking among (A) 90 kg male, (B) 70 kg male, and (C) 45 kg female. According to calibration curve, the average peak pressures can be obtained from “PD” as (A) 321 kPa, (B) 394 kPa, (C) 259 kPa, which indicate relatively good agreement with literature data.<sup>84</sup>

Meanwhile, the details of force-sensing peaks in the time domain also specify the features of walking paces. The time interval between the two closest separation and contact signals indicates the swing time of the leg in the air, and the time interval between “PA/PB” (forefoot) and “PC/PD” (heel) shows the time delay of these two contacts. For a specific sensor, the interval within two positive or negative peaks gives the duration of a single step cycle. In addition, the relative weight can be obtained through the different output voltages under the same test scenario, as shown in Figure 6e. Hence, by crosschecking the walking paces between two feet, together with a relative accurate determination of the received force, the S<sup>2</sup>-sock can support more information to the diagnosis of physical defects or training consultation, such as the healthcare application of PD mentioned previously. Unlike standard clinic diagnosis which requires accurate and precise determination of contact forces and positions, S<sup>2</sup>-sock can provide enough sensory information with the aid of piezoelectric sensors for personal applications with long-term stability of PZT chips (see Figure S9 in Supporting Information). On the basis of Figure 6d, it is also noticed that the pressure signals obtained from two adjacent PZT sensors will not vary a lot. The fewer PZT chips are desirable to ensure the comfortability and low cost while maintaining the hybrid and diversified functions, *i.e.*, sweat sensing, and activity monitoring.

For practical applications, both of TENG and PZT sensor requires further data processing to obtain useful information from preliminary output signals. Thus, machine learning approach will be a favorable tool to perform such an analysis job, such as feature extraction, normalization, and classification.<sup>81</sup> Especially for the S<sup>2</sup>-sock, shoe variation alters the output signals of both TENG and PZT sensors, and either waveform or amplitude may change. And human activities are not possible to be maintained with absolute consistency. Therefore, a specific recognition system must to be trained through machine learning for assessing the data set.

## CONCLUSIONS

In general, by using the PEDOT:PSS coated conventional cotton textile, we successfully developed a S<sup>2</sup>-sock which can realize the walking-pattern recognition and motion-tracking functions for smart home applications. We provided the preliminary data of individual and environmental variations to investigate and verify the stability of TENG sensors. Gait analysis was achieved by analyzing signals from TENG sock with a featured multisectional pattern. While these functions could only be achieved by insoles with integrated additional sensors previously. PZT chips with the minimum amount can provide the gait pattern information as well. The triboelectric output of TENG sock against the variation of sweat level was analyzed, and 80% decrement of output voltage was obtained as the amount of absorbed sweat reached 0.9 g. As the key of sensing is the waveform pattern instead of amplitude, sweat will not affect the function at a transient state. Meanwhile, this TENG sock with a sensitivity of 0.06 V/N is proven to reveal the impact force determined by contact speed after the calibration of piezoresistive and PZT sensors. However, assuming the same participant is walking with the same style, the difference of extra loading weight will not affect the output amplitude, but the foot size among different participants can cause the variations of amplitude. This work reports a smart sock with great potential to be a self-powered and self-functional platform where the triboelectric output power of 1.71 mW, *i.e.*, power density of 11  $\mu\text{W}/\text{cm}^2$ , was also achieved in 2 Hz jumping. The measured piezoelectric power density is 128  $\mu\text{W}/\text{cm}^2$  for PZT chips. Basically, the pure TENG S<sup>2</sup>-sock demonstrated diversified functions including energy harvesting, walking pattern recognition, motion tracking, gait sensing, as well as sweat sensing, and further explorations may allow us to obtain more comprehensive information which is beneficial for smart home, sports monitoring, healthcare, *etc.*

## METHODS

**Fabrication of PEDOT:PSS-Coated Sock.** Poly(3,4-ethylenedioxythiophene) polystyrenesulfonate (PEDOT:PSS) solution was prepared from purchased powder (Heraeus, Clevios PH 1000) and doped with 5 wt % dimethyl sulfoxide (DMSO) solution (Sigma-Aldrich) to enhance conductivity. Then the solution was mixed thoroughly by magnetic stirring for 15–20 min. After mixing, the solution was further diluted into 20 wt % solution (see the optimized results of Figure S1 in the Supporting Information) with DI water. A pure cotton sock was then immersed into the diluted PEDOT:PSS solution for 15 min. After completed absorption, the sock was dried in the oven (4 h, 75 °C).

**Fabrication of Thin PZT Chip.** A 1.5 cm × 1.5 cm lead zirconate titanate (PZT) ceramic (Fuji Ceramics Inc., C-6) and 50  $\mu\text{m}$  beryllium copper foil were polished at first. After sputtering of Cr/Au (Cr: 20 nm, 100 W, 2 min; Au: 200 nm, 100 W, 5 min) as bottom electrode on one side (bottom surface) of PZT, it is bonded with copper foil by conductive silver paste and baked in vacuum oven (3.5 h at 175 °C).

Then the bonded PZT chip was thinned down to 20  $\mu\text{m}$  by chemical mechanical polishing. The top Au electrode was then sputtered with the same approach. After that, the as-fabricated thin PZT chip was further diced to 5 mm × 5 mm size by laser cutting. The wires were then connected to both top and bottom electrodes and followed by the encapsulation of PZT chip using polyimide tape (3M).

**Characterization.** For both TENG sock and PZT chip, the open-circuit voltage and short-circuit current were measured by oscilloscope (Agilent, InfiniVision, DSO-X 3034A) connected with high-impedance electrometer (Keithley 6514). Calibration of the output voltage against force for PZT chip was conducted by force gauge (Mecmesin, MultiTest 2.5-i) and for TENG sensor was measured by “FlexiForce” resistive force sensor (A201). The calibration data of the “FlexiForce” sensor is shown in Figure S3. Temperature and humidity were controlled by heater/cooler and humidifier.

**Measurement of Output Power.** The contact-separation mode was used by connecting the sock with PTFE film. For wearing shoes, the PTFE film was attached onto the inner surface of shoes. For bare sock, the PTFE film was placed on the ground. A 100 M $\Omega$  probe was connected to the oscilloscope for measurement, and the external loading resistance was connected in parallel and varied from 0.5 to 148 M $\Omega$ .

**Measurement of Walking Pattern and Motion Tracking.** The contact-separation mode was used for comparing the performance between fully coated S<sup>2</sup>-sock and original sock. For both walking pattern and motion tracking, the output signals were obtained from PTFE side with a single-electrode mode.

**Measurement of Gait Analysis.** The single-electrode mode was applied by collecting output signals from the designed areas of the multisectional coated S<sup>2</sup>-sock, without connecting the electrode from PTFE.

**Measurement of Sweat Sensor.** A 0.9 wt % (0.1538 mol/L) sodium chloride solution (the ion concentrations of real sweat vary from 0.02 to 0.08 mol/L for sodium and 0.02 to 0.07 mol/L for chloride) was prepared in a spray bottle, and each spray delivered 0.1 g of solution. After uniform spraying, the output voltages of both TENG fabric and PZT sensor from regular activities (walking and jumping) were recorded.

## ASSOCIATED CONTENT

### Supporting Information

The Supporting Information is available free of charge on the ACS Publications website at DOI: 10.1021/acsnano.8b08329.

Motion tracking (movie S1) (AVI)

Mimetic detection of Parkinson disease (movie S2) (AVI)

Gait sensing of pure contact (movie S3) (AVI)

Gait sensing of sliding motions (movie S4) (AVI)

Gait sensing of walking (movie S5) (AVI)

Figures S1–S10 providing the information on optimization of PEDOT:PSS concentration for coating the cotton textiles; comparison of open-circuit voltage of two triboelectric modes; calibration curve of “FlexiForce” resistive force sensor; characterization tests of TENG for changing temperature or humidity and relationship between output voltage and contact area of TENG; controlled test for output intensity and pattern recognition test under changing weight; motion tracking test with weight and humidity variations and stability test for Parkinson’s disease monitoring; comparison tests for TENG gait sensors with weight and humidity variations; stability test for TENG and PZT sensors; washability tests for PEDOT:PSS-coated cotton fabric (PDF)

## AUTHOR INFORMATION

## Corresponding Authors

\*E-mail: binyang@sjtu.edu.cn.

\*E-mail: chent@suda.edu.cn.

\*E-mail: elelc@nus.edu.sg.

ORCID 

Minglu Zhu: 0000-0001-6652-2133

Zhiran Yi: 0000-0002-8679-8302

Bin Yang: 0000-0001-7948-3823

Tao Chen: 0000-0003-3550-2310

Chengkuo Lee: 0000-0002-8886-3649

## Author Contributions

M.Z. and Q.S. contributed equally to this work.

## Notes

The authors declare no competing financial interest.

## ACKNOWLEDGMENTS

This work was supported by HIFES Seed Funding-2017-01 grant (R-263-501-012-133) "Hybrid Integration of Flexible Power Source and Pressure Sensors" at the National University of Singapore; Agency for Science, Technology and Research (A\*STAR), Singapore and Narodowe Centrum Badań i Rozwoju (NCBR), Poland Joint Grant (R-263-000-C91-305) "Chip-Scale MEMS Micro-Spectrometer for Monitoring Harsh Industrial Gases".

## REFERENCES

- Wang, X.; Zhang, Y.; Zhang, X.; Huo, Z.; Li, X.; Que, M.; Peng, Z.; Wang, H.; Pan, C. A Highly Stretchable Transparent Self-Powered Triboelectric Tactile Sensor with Metallized Nanofibers for Wearable Electronics. *Adv. Mater.* **2018**, *30*, 1–8.
- Yang, P. K.; Lin, Z. H.; Pradel, K. C.; Lin, L.; Li, X.; Wen, X.; He, J. H.; Wang, Z. L. Paper-Based Origami Triboelectric Nanogenerators and Self-Powered Pressure Sensors. *ACS Nano* **2015**, *9*, 901–907.
- Wu, C.; Wang, X.; Lin, L.; Guo, H.; Wang, Z. L. Paper-Based Triboelectric Nanogenerators Made of Stretchable Interlocking Kirigami Patterns. *ACS Nano* **2016**, *10*, 4652–4659.
- Yang, P. K.; Lin, L.; Yi, F.; Li, X.; Pradel, K. C.; Zi, Y.; Wu, C. I.; He, J. H.; Zhang, Y.; Wang, Z. L. A Flexible, Stretchable and Shape-Adaptive Approach for Versatile Energy Conversion and Self-Powered Biomedical Monitoring. *Adv. Mater.* **2015**, *27*, 3817–3824.
- Fan, J. A.; Yeo, W. H.; Su, Y.; Hattori, Y.; Lee, W.; Jung, S. Y.; Zhang, Y.; Liu, Z.; Cheng, H.; Falgout, L.; Bajema, M.; Coleman, T.; Gregoire, D.; Larsen, R. J.; Huang, Y.; Rogers, J. A. Fractal Design Concepts for Stretchable Electronics. *Nat. Commun.* **2014**, *5*, 1–8.
- Bariya, M.; Nyein, H. Y. Y.; Javey, A. Wearable Sweat Sensors. *Nat. Electron.* **2018**, *1*, 160–171.
- Gao, W.; Emaminejad, S.; Nyein, H. Y. Y.; Challa, S.; Chen, K.; Peck, A.; Fahad, H. M.; Ota, H.; Shiraki, H.; Kiriya, D.; Lien, D.-H.; Brooks, G. A.; Davis, R. W.; Javey, A. Fully Integrated Wearable Sensor Arrays for Multiplexed *In Situ* Perspiration Analysis. *Nature* **2016**, *529*, 509–514.
- Jia, W.; Bandodkar, A. J.; Valdés-Ramírez, G.; Windmiller, J. R.; Yang, Z.; Ramírez, J.; Chan, G.; Wang, J. Electrochemical Tattoo Biosensors for Real-Time Noninvasive Lactate Monitoring in Human Perspiration. *Anal. Chem.* **2013**, *85*, 6553–6560.
- Kim, J.; Lee, M.; Shim, H. J.; Ghaffari, R.; Cho, H. R.; Son, D.; Jung, Y. H.; Soh, M.; Choi, C.; Jung, S.; Chu, K.; Jeon, D.; Lee, S. T.; Kim, J. H.; Choi, S. H.; Hyeon, T.; Kim, D. H. Stretchable Silicon Nanoribbon Electronics for Skin Prosthesis. *Nat. Commun.* **2014**, *5*, 1–11.
- Tee, B. C.-K.; Chortos, A.; Berndt, A.; Nguyen, A. K.; Tom, A.; McGuire, A.; Lin, Z. C.; Tien, K.; Bae, W.-G.; Wang, H.; Mei, P.; Chou, H.-H.; Cui, B.; Deisseroth, K.; Ng, T. N.; Bao, Z. A Skin-Inspired

Organic Digital Mechanoreceptor. *Science (Washington, DC, U. S.)* **2015**, *350*, 313–316.

(11) Gao, Y.; Ota, H.; Schaler, E. W.; Chen, K.; Zhao, A.; Gao, W.; Fahad, H. M.; Leng, Y.; Zheng, A.; Xiong, F.; Zhang, C.; Tai, L. C.; Zhao, P.; Fearing, R. S.; Javey, A. Wearable Microfluidic Diaphragm Pressure Sensor for Health and Tactile Touch Monitoring. *Adv. Mater.* **2017**, *29*, 1–8.

(12) Choi, M. K.; Yang, J.; Kang, K.; Kim, D. C.; Choi, C.; Park, C.; Kim, S. J.; Chae, S. I.; Kim, T. H.; Kim, J. H.; Hyeon, T.; Kim, D. H. Wearable Red-Green-Blue Quantum Dot Light-Emitting Diode Array Using High-Resolution Intaglio Transfer Printing. *Nat. Commun.* **2015**, *6*, 1–8.

(13) Tricoli, A.; Nasiri, N.; De, S. Wearable and Miniaturized Sensor Technologies for Personalized and Preventive Medicine. *Adv. Funct. Mater.* **2017**, *27*, 1–19.

(14) Ouyang, H.; Tian, J.; Sun, G.; Zou, Y.; Liu, Z.; Li, H.; Zhao, L.; Shi, B.; Fan, Y.; Fan, Y.; Wang, Z. L.; Li, Z. Self-Powered Pulse Sensor for Antidiastole of Cardiovascular Disease. *Adv. Mater.* **2017**, *29*, 1–10.

(15) Jiang, Q.; Wu, C.; Wang, Z.; Wang, A. C.; He, J. H.; Wang, Z. L.; Alshareef, H. N. MXene Electrochemical Microsupercapacitor Integrated with Triboelectric Nanogenerator as a Wearable Self-Charging Power Unit. *Nano Energy* **2018**, *45*, 266–272.

(16) Zhang, F.; Zang, Y.; Huang, D.; Di, C. A.; Zhu, D. Flexible and Self-Powered Temperature-Pressure Dual-Parameter Sensors Using Microstructure-Frame-Supported Organic Thermoelectric Materials. *Nat. Commun.* **2015**, *6*, 1–10.

(17) Leung, S. F.; Ho, K. T.; Kung, P. K.; Hsiao, V. K. S.; Alshareef, H. N.; Wang, Z. L.; He, J. H. A Self-Powered and Flexible Organometallic Halide Perovskite Photodetector with Very High Detectivity. *Adv. Mater.* **2018**, *30*, 1–8.

(18) Lee, J. H.; Lee, K. Y.; Gupta, M. K.; Kim, T. Y.; Lee, D. Y.; Oh, J.; Ryu, C.; Yoo, W. J.; Kang, C. Y.; Yoon, S. J.; Yoo, J. B.; Kim, S. W. Highly Stretchable Piezoelectric-Pyroelectric Hybrid Nanogenerator. *Adv. Mater.* **2014**, *26*, 765–769.

(19) Chen, H.; Song, Y.; Cheng, X.; Zhang, H. Self-Powered Electronic Skin Based on the Triboelectric Generator. *Nano Energy* **2019**, *56*, 252–268.

(20) Zhang, Q.; Zhang, Z.; Liang, Q.; Gao, F.; Yi, F.; Ma, M.; Liao, Q.; Kang, Z.; Zhang, Y. Green Hybrid Power System Based on Triboelectric Nanogenerator for Wearable/Portable Electronics. *Nano Energy* **2019**, *55*, 151–163.

(21) Hu, Y.; Zheng, Z. Progress in Textile-Based Triboelectric Nanogenerators for Smart Fabrics. *Nano Energy* **2019**, *56*, 16–24.

(22) Choi, W.; Yun, I.; Jeung, J.; Park, Y. S.; Cho, S.; Kim, D. W.; Kang, I. S.; Chung, Y.; Jeong, U. Stretchable Triboelectric Multimodal Tactile Interface Simultaneously Recognizing Various Dynamic Body Motions. *Nano Energy* **2019**, *56*, 347–356.

(23) Paosangthong, W.; Torah, R.; Beeby, S. Recent Progress on Textile-Based Triboelectric Nanogenerators. *Nano Energy* **2019**, *55*, 401–423.

(24) Persano, L.; Dagdeviren, C.; Su, Y.; Zhang, Y.; Girardo, S.; Pisignano, D.; Huang, Y.; Rogers, J. A. High Performance Piezoelectric Devices Based on Aligned Arrays of Nanofibers of Poly(Vinylidene fluoride-Co-Trifluoroethylene). *Nat. Commun.* **2013**, *4*, 1610–1633.

(25) Chen, J.; Huang, Y.; Zhang, N.; Zou, H.; Liu, R.; Tao, C.; Fan, X.; Wang, Z. L. Micro-Cable Structured Textile for Simultaneously Harvesting Solar and Mechanical Energy. *Nat. Energy* **2016**, *1*, 1–8.

(26) Pu, X.; Li, L.; Liu, M.; Jiang, C.; Du, C.; Zhao, Z.; Hu, W.; Wang, Z. L. Wearable Self-Charging Power Textile Based on Flexible Yarn Supercapacitors and Fabric Nanogenerators. *Adv. Mater.* **2016**, *28*, 98–105.

(27) Gong, X.; Li, S.; Lee, P. S. A Fiber Asymmetric Supercapacitor Based on FeOOH/PPy on Carbon Fibers as an Anode Electrode with High Volumetric Energy Density for Wearable Applications. *Nanoscale* **2017**, *9*, 10794–10801.

(28) Chen, L.; Shi, Q.; Sun, Y.; Nguyen, T.; Lee, C.; Soh, S. Controlling Surface Charge Generated by Contact Electrification: Strategies and Applications. *Adv. Mater.* **2018**, *30*, 1–15.

- (29) Lai, Y.-C.; Deng, J.; Zhang, S. L.; Niu, S.; Guo, H.; Wang, Z. L. Single-Thread-Based Wearable and Highly Stretchable Triboelectric Nanogenerators and Their Applications in Cloth-Based Self-Powered Human-Interactive and Biomedical Sensing. *Adv. Funct. Mater.* **2017**, *27*, 1604462.
- (30) Wu, H.; Guo, H.; Su, Z.; Shi, M.; Chen, X.; Cheng, X.; Han, M.; Zhang, H. A Fabric-Based Self-Powered Noncontact Smart Gloves for Gesture Recognition. *J. Mater. Chem. A* **2018**, *6*, 20277–20288.
- (31) Lee, J.; Kwon, H.; Seo, J.; Shin, S.; Koo, J. H.; Pang, C.; Son, S.; Kim, J. H.; Jang, Y. H.; Kim, D. E.; Lee, T. Conductive Fiber-Based Ultrasensitive Textile Pressure Sensor for Wearable Electronics. *Adv. Mater.* **2015**, *27*, 2433–2439.
- (32) Cao, R.; Pu, X.; Du, X.; Yang, W.; Wang, J.; Guo, H.; Zhao, S.; Yuan, Z.; Zhang, C.; Li, C.; Wang, Z. L. Screen-Printed Washable Electronic Textiles as Self-Powered Touch/Gesture Tribo-Sensors for Intelligent Human-Machine Interaction. *ACS Nano* **2018**, *12*, 5190–5196.
- (33) He, T.; Shi, Q.; Wang, H.; Wen, F.; Chen, T.; Ouyang, J.; Lee, C. Beyond Energy Harvesting - Multi-Functional Triboelectric Nanosensors on a Textile. *Nano Energy* **2019**, *57*, 338–352.
- (34) Yu, A.; Pu, X.; Wen, R.; Liu, M.; Zhou, T.; Zhang, K.; Zhang, Y.; Zhai, J.; Hu, W.; Wang, Z. L. Core-Shell-Yarn-Based Triboelectric Nanogenerator Textiles as Power Cloths. *ACS Nano* **2017**, *11*, 12764–12771.
- (35) Lin, Z.; Yang, J.; Li, X.; Wu, Y.; Wei, W.; Liu, J.; Chen, J.; Yang, J. Large-Scale and Washable Smart Textiles Based on Triboelectric Nanogenerator Arrays for Self-Powered Sleeping Monitoring. *Adv. Funct. Mater.* **2018**, *28*, 1–7.
- (36) Wang, Z. L.; Lin, L.; Chen, J.; Niu, S.; Zi, Y. *Triboelectric Nanogenerators*; Springer International Publishing, 2016.
- (37) Jeon, S. B.; Seol, M. L.; Kim, D.; Park, S. J.; Choi, Y. K. Self-Powered Ion Concentration Sensor with Triboelectricity from Liquid–Solid Contact Electrification. *Adv. Electron. Mater.* **2016**, *2*, 1–7.
- (38) Wang, H.; Wu, H.; Hasan, D.; He, T.; Shi, Q.; Lee, C. Self-Powered Dual-Mode Amenity Sensor Based on the Water-Air Triboelectric Nanogenerator. *ACS Nano* **2017**, *11*, 10337–10346.
- (39) Xiong, J.; Lin, M. F.; Wang, J.; Gaw, S. L.; Parida, K.; Lee, P. S. Wearable All-Fabric-Based Triboelectric Generator for Water Energy Harvesting. *Adv. Energy Mater.* **2017**, *7*, 1–10.
- (40) Dagdeviren, C.; Yang, B. D.; Su, Y.; Tran, P. L.; Joe, P.; Anderson, E.; Xia, J.; Doraiswamy, V.; Dehdashti, B.; Feng, X.; Lu, B.; Poston, R.; Khalpey, Z.; Ghaffari, R.; Huang, Y.; Slepian, M. J.; Rogers, J. A. Conformal Piezoelectric Energy Harvesting and Storage from Motions of the Heart, Lung, and Diaphragm. *Proc. Natl. Acad. Sci. U. S. A.* **2014**, *111*, 1927–1932.
- (41) Dagdeviren, C.; Su, Y.; Joe, P.; Yona, R.; Liu, Y.; Kim, Y. S.; Huang, Y.; Damadoran, A. R.; Xia, J.; Martin, L. W.; Huang, Y.; Rogers, J. A. Conformable Amplified Lead Zirconate Titanate Sensors with Enhanced Piezoelectric Response for Cutaneous Pressure Monitoring. *Nat. Commun.* **2014**, *5*, 1–10.
- (42) Shibata, K.; Wang, R.; Tou, T.; Koruza, J. Applications of Lead-Free Piezoelectric Materials. *MRS Bull.* **2018**, *43*, 612–616.
- (43) Park, D. Y.; Joe, D. J.; Kim, D. H.; Park, H.; Han, J. H.; Jeong, C. K.; Park, H.; Park, J. G.; Joung, B.; Lee, K. J. Self-Powered Real-Time Arterial Pulse Monitoring Using Ultrathin Epidermal Piezoelectric Sensors. *Adv. Mater.* **2017**, *29*, 1–9.
- (44) Damjanovic, D.; Rossetti, G. A. Strain Generation and Energy-Conversion Mechanisms in Lead-Based and Lead-Free Piezoceramics. *MRS Bull.* **2018**, *43*, 588–594.
- (45) Kim, S. G.; Priya, S.; Kanno, I. Piezoelectric MEMS for Energy Harvesting. *MRS Bull.* **2012**, *37*, 1039–1050.
- (46) Rödiger, T.; Schönecker, A.; Gerlach, G. A Survey on Piezoelectric Ceramics for Generator Applications. *J. Am. Ceram. Soc.* **2010**, *93*, 901–912.
- (47) Baek, S. H.; Rzechowski, M. S.; Aksyuk, V. A. Giant Piezoelectricity in PMN-PT Thin Films: Beyond PZT. *MRS Bull.* **2012**, *37*, 1022–1029.
- (48) Wu, J. M.; Lee, C. C.; Lin, Y. H. High Sensitivity Wrist-Worn Pulse Active Sensor Made from Tellurium Dioxide Microwires. *Nano Energy* **2015**, *14*, 102–110.
- (49) Wang, X.; Yang, B.; Liu, J.; Zhu, Y.; Yang, C.; He, Q. A Flexible Triboelectric-Piezoelectric Hybrid Nanogenerator Based on P(VDF-TrFE) Nanofibers and PDMS/MWCNT for Wearable Devices. *Sci. Rep.* **2016**, *6*, 1–10.
- (50) Li, X.; Lin, Z.-H.; Cheng, G.; Wen, X.; Liu, Y.; Niu, S.; Wang, Z. L. 3D Fiber-Based Hybrid Nanogenerator for Energy Harvesting and as a Self-Powered Pressure Sensor. *ACS Nano* **2014**, *8*, 10674–10681.
- (51) Zheng, Q.; Shi, B.; Li, Z.; Wang, Z. L. Recent Progress on Piezoelectric and Triboelectric Energy Harvesters in Biomedical Systems. *Adv. Sci.* **2017**, *4*, 1–23.
- (52) Lee, K. Y.; Gupta, M. K.; Kim, S. W. Transparent Flexible Stretchable Piezoelectric and Triboelectric Nanogenerators for Powering Portable Electronics. *Nano Energy* **2015**, *14*, 139–160.
- (53) Kim, J.; Lee, J. H.; Ryu, H.; Lee, J. H.; Khan, U.; Kim, H.; Kwak, S. S.; Kim, S. W. High-Performance Piezoelectric Pyroelectric, and Triboelectric Nanogenerators Based on P(VDF-TrFE) with Controlled Crystallinity and Dipole Alignment. *Adv. Funct. Mater.* **2017**, *27*, 1–8.
- (54) Wang, X.; Yang, B.; Liu, J.; Yang, C. A Transparent and Biocompatible Single-Friction-Surface Triboelectric and Piezoelectric Generator and Body Movement Sensor. *J. Mater. Chem. A* **2017**, *5*, 1176–1183.
- (55) Tao, W.; Liu, T.; Zheng, R.; Feng, H. Gait Analysis Using Wearable Sensors. *Sensors* **2012**, *12*, 2255–2283.
- (56) Henriksen, M.; Lund, H.; Moe-Nilssen, R.; Bliddal, H.; Danneskiold-Samsøe, B. Test-Retest Reliability of Trunk Accelerometric Gait Analysis. *Gait Posture* **2004**, *19*, 288–297.
- (57) Moe-Nilssen, R.; Helbostad, J. L. Estimation of Gait Cycle Characteristics by Trunk Accelerometry. *J. Biomech.* **2004**, *37*, 121–126.
- (58) Han, Y.; Yi, F.; Jiang, C.; Dai, K.; Xu, Y.; Wang, X.; You, Z. Self-Powered Gait Pattern-Based Identity Recognition by a Soft and Stretchable Triboelectric Band. *Nano Energy* **2019**, *56*, 516–523.
- (59) Niu, S.; Wang, X.; Yi, F.; Zhou, Y. S.; Wang, Z. L. A Universal Self-Charging System Driven by Random Biomechanical Energy for Sustainable Operation of Mobile Electronics. *Nat. Commun.* **2015**, *6*, 8975.
- (60) Kim, K. N.; Lee, J. P.; Lee, S. H.; Lee, S. C.; Baik, J. M. Ergonomically Designed Replaceable and Multifunctional Triboelectric Nanogenerator for a Uniform Contact. *RSC Adv.* **2016**, *6*, 88526–88530.
- (61) Jung, W. S.; Lee, M. J.; Kang, M. G.; Moon, H. G.; Yoon, S. J.; Baek, S. H.; Kang, C. Y. Powerful Curved Piezoelectric Generator for Wearable Applications. *Nano Energy* **2015**, *13*, 174–181.
- (62) Zhu, G.; Bai, P.; Chen, J.; Lin, W.; Wang, Z. Power-Generating Shoe Insole Based on Triboelectric Nanogenerators for Self-Powered Consumer Electronics. *Nano Energy* **2013**, *2*, 688–692.
- (63) Jao, Y. T.; Yang, P. K.; Chiu, C. M.; Lin, Y. J.; Chen, S. W.; Choi, D.; Lin, Z. H. A Textile-Based Triboelectric Nanogenerator with Humidity-Resistant Output Characteristic and Its Applications in Self-Powered Healthcare Sensors. *Nano Energy* **2018**, *50*, 513–520.
- (64) Chen, C. H.; Lee, P. W.; Tsao, Y. H.; Lin, Z. H. Utilization of Self-Powered Electrochemical Systems: Metallic Nanoparticle Synthesis and Lactate Detection. *Nano Energy* **2017**, *42*, 241–248.
- (65) Wang, S.; Xie, G.; Tai, H.; Su, Y.; Yang, B.; Zhang, Q.; Du, X.; Jiang, Y. Ultrasensitive Flexible Self-Powered Ammonia Sensor Based on Triboelectric Nanogenerator at Room Temperature. *Nano Energy* **2018**, *51*, 231–240.
- (66) Cui, S.; Zheng, Y.; Zhang, T.; Wang, D.; Zhou, F.; Liu, W. Self-Powered Ammonia Nanosensor Based on the Integration of the Gas Sensor and Triboelectric Nanogenerator. *Nano Energy* **2018**, *49*, 31–39.
- (67) Wang, H.; Pastorin, G.; Lee, C. Toward Self-Powered Wearable Adhesive Skin Patch with Bendable Microneedle Array for Transdermal Drug Delivery. *Adv. Sci.* **2016**, *3*, 1–10.
- (68) Wang, C.; Hu, K.; Li, W.; Wang, H.; Li, H.; Zou, Y.; Zhao, C.; Li, Z.; Yu, M.; Tan, P.; Li, Z. Wearable Wire-Shaped Symmetric

Supercapacitors Based on Activated Carbon-Coated Graphite Fibers. *ACS Appl. Mater. Interfaces* **2018**, *10*, 34302–34310.

(69) Gu, G. Q.; Han, C. B.; Tian, J. J.; Lu, C. X.; He, C.; Jiang, T.; Li, Z.; Wang, Z. L. Antibacterial Composite Film-Based Triboelectric Nanogenerator for Harvesting Walking Energy. *ACS Appl. Mater. Interfaces* **2017**, *9*, 11882–11888.

(70) Chen, T.; Zhao, M.; Shi, Q.; Yang, Z.; Liu, H.; Sun, L.; Ouyang, J.; Lee, C. Novel Augmented Reality Interface Using a Self-Powered Triboelectric Based Virtual Reality 3D-Control Sensor. *Nano Energy* **2018**, *51*, 162–172.

(71) Lee, S.; Wang, H.; Shi, Q.; Dhakar, L.; Wang, J.; Thakor, N. V.; Yen, S. C.; Lee, C. Development of Battery-Free Neural Interface and Modulated Control of Tibialis Anterior Muscle *via* Common Peroneal Nerve Based on Triboelectric Nanogenerators (TENGS). *Nano Energy* **2017**, *33*, 1–11.

(72) Ouyang, J.; Chu, C. W.; Chen, F. C.; Xu, Q.; Yang, Y. High-Conductivity Poly(3,4-Ethylenedioxythiophene):Poly(Styrene Sulfonate) Film and Its Application in Polymer Optoelectronic Devices. *Adv. Funct. Mater.* **2005**, *15*, 203–208.

(73) Ding, Y.; Invernale, M. A.; Sotzing, G. A. Conductivity Trends of Pedot-Pss Impregnated Fabric and the Effect of Conductivity on Electrochromic Textile. *ACS Appl. Mater. Interfaces* **2010**, *2*, 1588–1593.

(74) Liu, L.; Pan, J.; Chen, P.; Zhang, J.; Yu, X.; Ding, X.; Wang, B.; Sun, X.; Peng, H. A Triboelectric Textile Templated by a Three-Dimensionally Penetrated Fabric. *J. Mater. Chem. A* **2016**, *4*, 6077–6083.

(75) Zhang, L.; Yu, Y.; Eyer, G. P.; Suo, G.; Kozik, L. A.; Fairbanks, M.; Wang, X.; Andrew, T. L. All-Textile Triboelectric Generator Compatible with Traditional Textile Process. *Adv. Mater. Technol.* **2016**, *1*, 1600147.

(76) Chen, M.; Li, X.; Lin, L.; Du, W.; Han, X.; Zhu, J.; Pan, C.; Wang, Z. L. Triboelectric Nanogenerators as a Self-Powered Motion Tracking System. *Adv. Funct. Mater.* **2014**, *24*, 5059–5066.

(77) Casamassima, F.; Ferrari, A.; Milosevic, B.; Ginis, P.; Farella, E.; Rocchi, L. A Wearable System for Gait Training in Subjects with Parkinson's Disease. *Sensors* **2014**, *14*, 6229–6246.

(78) Kimmeskamp, S.; Hennig, E. M. Heel to Toe Motion Characteristics in Parkinson Patients during Free Walking. *Clin. Biomech.* **2001**, *16*, 806–812.

(79) Moore, S. T.; MacDougall, H. G.; Ondo, W. G. Ambulatory Monitoring of Freezing of Gait in Parkinson's Disease. *J. Neurosci. Methods* **2008**, *167*, 340–348.

(80) Nieuwboer, A.; Dom, R.; De Weerd, W.; Desloovere, K.; Fieuws, S.; Broens-Kaucsik, E. Abnormalities of the Spatiotemporal Characteristics of Gait at the Onset of Freezing in Parkinson's Disease. *Mov. Disord.* **2001**, *16*, 1066–1075.

(81) Mason, J. E.; Traoré, I.; Woungang, I. *Machine Learning Techniques for Bioinformatics*; Springer International Publishing, 2016.

(82) Redd, C. B.; Bamberg, S. J. M. A Wireless Sensory Feedback Device for Real-Time Gait Feedback and Training. *IEEE/ASME Trans. Mechatronics* **2012**, *17*, 425–433.

(83) Taylor, N. A.; Machado-Moreira, C. A. Regional Variations in Transepidermal Water Loss, Eccrine Sweat Gland Density, Sweat Secretion Rates and Electrolyte Composition in Resting and Exercising Humans. *Extrem. Physiol. Med.* **2013**, *2*, 4.

(84) Betts, R. P.; Franks, C. I.; Duckworth, T.; Burke, J. Static and Dynamic Foot-Pressure Measurements in Clinical Orthopaedics. *Med. Biol. Eng. Comput.* **1980**, *18*, 674–684.